# PROCESSING OF TEXTILE COMPOSITE MATERIALS BY USING SHAPE MEMORY ALLOYS

**Topel Zeren E.**[1], **Aksit A.**[1], **Ozyuzer L.**[2], **Aydogdu Y.**[3], **Erdogan U.H.**[1], **Kutlu B.**[1]
[1]*Dokuz Eylül University, Department of Textile Engineering, Buca, İzmir, TURKEY*
[2]*İzmir Institute of Technology, Department of Physics, Urla, İzmir, TURKEY*
[3]*Gazi University, Department of Physics, Ankara, TURKEY*
esratopel@gmail.com

**ABSTRACT**

Shape memory materials are stimulus-responsive materials and referred to use as smart materials/systems in the field of textiles in recent years. The aim of the study is to achieve shape memory fibers by adding the shape memory alloy particles (whiskers) into a polymer matrix. For this purpose, the whiskers are formed by thin films growth by magnetron sputtering. In our study targets were prepared with NiMnXY (X:Sn, Sb; Y:B)) metal in different atomic ratios and the sputtering parameters has been optimizing since the shape memory alloy thin films exhibited lower transformation temperatures around the body temperature.

**Key Words:** shape memory materials, shape memory alloys, thin film, magnetron sputtering, and smart textile

## 1. INTRODUCTION

Shape memory materials (SMMs) are one of the defined smart materials that capable of changing their properties by responding to environmental conditions. During the deformation of these materials, phase transformation occur which cause to change in the physical and mechanical properties of the material. These phase changes enable some new functions or adapt materials to changes in shape by the effect of external factors such as temperature, force, magnetic or electrical fields [1, 2]. Various alloys, polymers, ceramics, and gel structures are materials that have shape memory effect. In textile applications, shape memory polymers (SMPs) used as filament, foam or coating/lamination materials forms and shape memory alloys (SMAs) are used as wires and fiber coating [3-8]. Although, SMAs are used in limited textile applications, they are widely used in other industries ranging from the automotive to medical field [9-11].

SMAs are stimuli-responsive materials and able to change their structure under the right stimulus, based on two state phase: austenite and martensite. Austenite, called parent phase, is stable at high temperatures and the transformation occurs into martensite which is softer phase at lower temperatures. SMA begins to transform from martensite to austenite phase when it is heated. This transformation starts with austenite start temperature ($A_s$) and completes with austenite finish temperature ($A_f$). When SMA heated above $A_s$, it recovers into its original form. During the cooling, when it reaches to the martensite start temperature ($M_s$), the transformation returns martensite and completes when it reaches the martensite finish temperature ($M_f$). For martensitic transformations of SMAs, the shape memory effect (SME) is a distinctive property. The reverse transformation temperature is critical temperature for recovering the original shape upon heating after the alloy is deformed in low temperature [12,13].

The response is occurring slowly in the heat activated bulk SMAs and this heat must be removed between cycles but the duration of cooling process is so extended that slows down the reaction rate. When compared with bulk alloy, cycle time of the thin film SMAs is significantly decreased since the required thermal mass rate is reduced for the cooling process. Reduced

cycle time provides an advantage for the use of thin film alloys in applications. The studies show that magnetron sputtering is one of the main methods for thin film growth. The sputtering conditions such as gas pressure, power, substrate temperature, etc. and metallurgical factors are important in shape memory effect for thin films [14].

The aim of the study is to achieve shape memory fibers by adding the shape memory alloy particles (whiskers) into a polymer matrix. Thus, it is expected that the SMAs will be compatible for textile structure and their usage will be improved in textile applications. As it is different from the NiTi shape memory alloy thin films, which have been widely studied with film deposition, we used NiMn-based ferromagnetic alloys. Thin films are growth by magnetron sputtering and peeled off from the substrate to obtain whiskers. Targets used in magnetron sputtering were prepared in different atomic ratios with various compositions by using arc-melting method. Thus, shape memory alloyed thin films can be sputtered from these targets. The whiskers were doped into polyvinyl chloride (PVC) polymers in emulsion form to observe the shape recovering after reaching the suitable transformation temperature. Fundamental of this study is to produce thin films from SMAs with better shape memory effect (SME) and/or super elasticity (SE) properties.

## 2. MATERIALS AND METHODS

The alloy targets were prepared from Nickel (Ni, 99.8%), Manganese (Mn, 99.6%), Tin (Sn, 99.8%), Antimony (Sb, 99.5%), and Boron (B, 99.9%) metal powders with two different compositions by arc-melting method. The NiMn-based alloys are produced as $Ni_{50}Mn_{40-x}Sn_{10}B_x$ and $Ni_{50}Mn_{39-x}Sb_{11}B_x$ (at. %) (x=3) in compositions [15]. After arc-melting, the alloy materials were subjected to homogenization process under argon atmosphere at 900 $^oC$ for 17 hours and then rapidly cooled into salty-ice water. The transformation temperatures of target alloys were listed in Table 1.

**Table 1.** Properties of alloy targets

| **Temperatures ($^o$C)** | **$Ni_{50}Mn_{37}Sn_{10}B_3$** | **$Ni_{50}Mn_{36}Sb_{11}B_3$** |
|---|---|---|
| Martensite start temperature ($M_s$) | 91.06 | 36.32 |
| Martensite finish temperature ($M_f$) | 68.31 | 27.70 |
| Austenite start temperature ($A_s$) | 82.91 | 45.15 |
| Austenite finish temperature ($A_f$) | 105.84 | 57.68 |

According to their transformation temperature, alloys were used in two forms. The $Ni_{50}Mn_{37}Sn_{10}B_3$ target was used for sputtering thin film with better shape memory effect and lower transformation temperature. $Ni_{50}Mn_{37}Sn_{10}B_3$ thin films were deposited on glass substrate by RF magnetron sputtering system. Before the deposition, base pressure of chamber was lowered down to below $10^{-6}$ torr. During the sputtering, argon gas was fed into a chamber with 30 sccm flow and working pressure was kept at $10^{-4}$ torr. Power (40 and 80 Watt) and time (60, 90, and 120 minutes) were variables for sputtering of desired SMA thin films. After deposition, thin films were peeled off on the substrate and post annealing was performed at 450$^o$C for one hour under the vacuum condition. The $Ni_{50}Mn_{36}Sb_{11}B_3$ alloy was used for obtaining small particles by using agate mortar due to the lower transformation temperature for observing the effect of SMA particles from this alloys. This alloy material was pounded in an agate mortar and obtained particles size varies between 150 and 250 μm. NiMnSbB alloy was chosen because of the low transition temperatures as seen in Table 1.

Polyvinyl chloride (PVC) polymers in emulsion form was used to dope the alloy particles and be aimed to understand the shape memory effect of thin film particles and the particles obtained from NiMn-based alloys. These alloy particles were doped into the PVC polymer at a weight of 2% and homogenously mixed, and then applied onto a flat surface as a film form and dried at 160 $^{o}$C for 15 minutes. From these polymer films, strips were cut and shape-training studies were done. The samples were prepared in different shape and heat treated at 80 $^{o}$C for 20 minute and then cooled rapidly in water.

The film thickness was measured using surface profilometer (Veeco Dektak 150). The crystal structure of NiMnSnB thin films produced was performed by x-ray diffraction (XRD) using Philips X'Pert Pro diffractometer with Cu $K_{\alpha}$ radiation with a scanning speed of 0.08$^{o}$/s. The transformation temperatures of the samples were determined by using Perkin Elmer differential scanning calorimeter (DSC) at a temperature range between 0-400 $^{o}$C in a nitrogen environment with a 10 $^{o}$C/min heating-cooling ratio. Energy dispersive X-Ray spectroscopy (EDS) using EDX detector to analyze main components of produced thin films. The elemental contents were taken from three different points in each sample.

## 3. RESULTS AND DISCUSSIONS

### 3.1 Structural Properties of Thin Films

The thicknesses of the films were increased with the increase of deposition time. The film thicknesses were measured and found to be ~810, 1270, and 1800 nm, which were deposited as 60, 90, and 120 minutes respectively. Based on DSC curves of the NiMnSnB and NiMnSbB alloys, start and finish temperatures of both martensite and austenite were determined and shown in Table 1. It is clear that alloys showed reversible phase transformation. When the DSC curves of the NiMnSnB thin films were examined, each particle produced at 60, 90, and 120 minutes, only the austenite start and finish temperatures were found between ~310 $^{o}$C and ~350 $^{o}$C and reversible phase transformation was not observed on the thin film particles. Also, start and finish temperatures of austenite are much higher to use in our study. For this reason, optimizing post annealing and sputtering conditions of the thin films is ongoing to get lower transformation temperature.

Figure 1 shows the room temperature XRD pattern of the NiMnSnB thin films produced with 40W and 80W. XRD pattern of the thin films before annealing as shown on Figure 1a, one broad peak centered around $2\theta=43^{o}$ shows that the films are in amorphous structure. Annealing at 450 $^{o}$C increases the intensity and sharpness of the peak at $2\theta=42.72^{o}$ (220), that is signaling the crystallization of the $L2_1$ structure. Also, $2\theta=62.49$ (400) and $2\theta=79.21$ (422) fundamental peaks and the super-lattice peaks as $2\theta=25.92$ (111), and $2\theta=50.52$ (311) were detected. In addition, intensity and sharpness of the peaks, increase with the thickness of the film as seen on Figure 1b [15,16]. The XRD pattern of the NiMnSnB thin film deposited with 80W shows that the peaks sharpness at $2\theta=42.72^{o}$ (220) increase with applied power and also, the peak intensity and sharpness is clearly seen at 90 minutes' deposition time (Figure 1c).

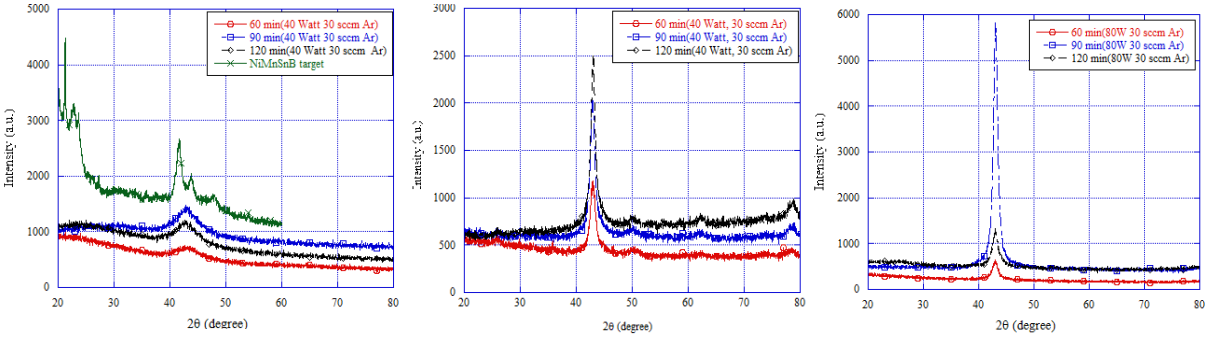


**a)** **b)** **c)**

**Figure 1.** XRD graphs of (40W) **a)** before annealing; **b)** after annealing; **c)** before annealing (80W)

EDS results showed that the main elemental composition of thin films was found to be close to the target alloy components. However, the exact composition of thin films could not be determined. According to these results Ni, Mn, and Sn were observed but the boron could not be detected by EDS.

### 3.2 Shape Memory Effect of Composites

The use of SMA particles of NiMnSbB and NiMnSnB particles formed by thin films into a polymer in emulsion form, aimed to produce shape memory materials which is adapted in textile structures. The one-way shape memory effect was observed in the doped PVCs samples depending on temperature as seen on Figure 2 and 3. The samples were dipped into water to observe their rapid response against thermal effect. As seen on the Figure 2a, samples were memorized the shape between the martensite start and finish temperature. In contrast, above the austenite start temperature, samples returned to their flat permanent shape. The PVC samples which were not doped with SMA particles were stayed in the training shape and could not be seen any response against to temperature as seen on Figure 2b.

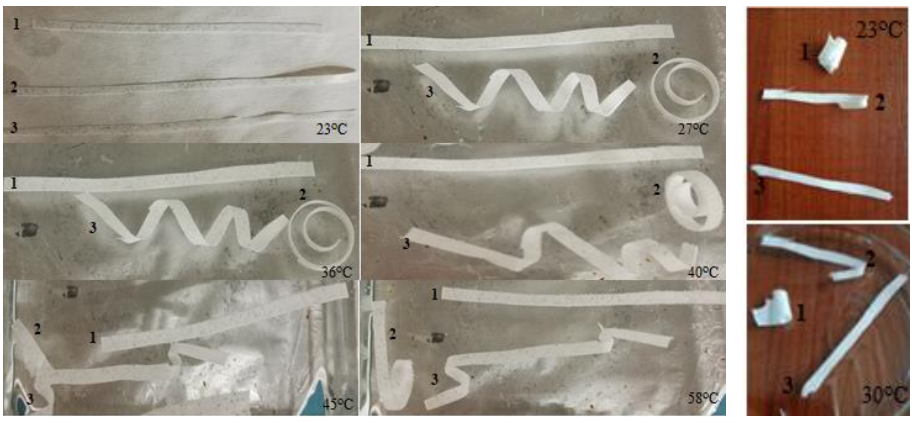


**a)** **b)**

**Figure 2.** Temperature-dependent shape change of **a)** NiMnSbB SMA particle doped PVCs; **b)** undoped PVCs

The samples were obtained by doping thin films into PVC as shown on Figure 3. In training process, the spiral form was given as temporary shape to the sample and it could be seen that sample memorized its temporary shape between 27 ºC and 40 ºC. Above the 45 ºC, the sample was started to recover the flat permanent shape.

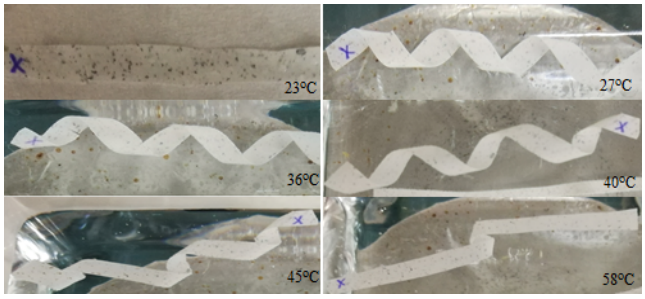


**Figure 3.** Temperature-dependent shape changing of NiMnSnB SMA thin film doped PVCs

## 4. CONCLUSIONS

The shape memory alloys were prepared according to defined metal elements and their combinations unlike the commercial and known products. Thus, the shape memory thin film production is occurred to use NiMn-based target. The magnetron sputtering is the most common method to growth thin film due to ease of control of the sputtering parameters. In this study, sputtering parameters and annealing temperatures are important factors for achieving the crystal structure and shape memory effect of thin films. According to these results, the future studies will be based on producing thin films which will be exhibited the reverse transformation effect with lower transformation temperatures. Thus, composite materials will be produced by combining the good shape memory characteristic of SMAs and a polymer material for textile applications.

## 5. ACKNOWLEDGEMENT

This study is financially supported by TUBITAK 1001-Scientific and Technological Research Projects Funding Program under project number 117M741.

## 6. REFERENCES

1. Arun D I., Chakravarthy P., Arockiakumar R, Santhosh B., *Shape memory materials*, CRC Press/Taylor & Francis Group, Boca Raton, 2018, 1-50.
2. Sun L, Huang W.M, Ding Z, Zhao Y., Wang C.C, Purnavali H, Tang C, Stimulus-responsive shape memory materials: A review, *Materials and Design*, 2012, 33, 577-640.
3. Lam Po Tang, S. and Stylios, G. K., An Overview of Smart Technologies for Clothing Design and Engineering, *International Journal of Clothing Science and Technology*, 2006, 18(2), 108-128.
4. Stylios, G. K. and Wan, T., Shape memory training for smart fabrics, *Transactions of the Institute of Measurement and Control*, 2007, 29, 3/4, 321–336.
5. Hu J., Zhu Y., Huang H, and Lu J., Recent Advances in Shape–Memory Polymers: Structure, mechanism, functionality, modeling and applications, *Progress in Polymer Science*, 2012, 37, 1720– 1763.
6. Cha D., Kim H.Y., Lee K.H., Jung Y.C., Cho J.W, Chun B.C., Electrospun Nonwovens of Shape-Memory Polyurethane Block Copolymers, *Journal of Applied Polymer Science*, 2005, 96, 460 – 465.
7. Cabral I, Souto AP, Carvalho H. and Cunha J., Exploring geometric morphology in shape memory textiles: design of dynamic light filters, *Textile Research Journal*, 2015, 85(18), 1919–1933.

8. Chan Vili Y.Y.F., Investigating Smart Textiles Based on Shape Memory Materials, *Textile Research Journal*, 2007, 77(5): 290–300.
9. Hu, J., *Shape Memory Polymers and Textiles*, Woodhead Publishing Limited, CRC Press, ABD, 2007.
10. Petrini L. and Migliavacca F., Review Article Biomedical Applications of Shape Memory Alloys, *Journal of Metallurgy*, 2011, Article ID 501483, 15 pages.
11. Fischer H., Vogel B. and Welle A., Applications of shape memory alloys in medical instruments, *Minimally Invasive Therapy & Allied Technologies*, 2004, 13(4), 248-253.
12. Mohd Jani J, Leary M, Subic A, Gibson MA, A review of shape memory alloy research, applications and opportunities, *Materials and Design*, 2014, 56, 1078-1113.
13. Otsuka K and Wayman C.M, *Shape memory Materials*, Cambridge University Press, 1999, 1-27.
14. Wei Z.G., Sandström R., Review Shape-memory materials and hybrid composites for smart systems Part I Shape-memory materials, *Journal of Materials Science*, 1998, 33, 3743-3762.
15. Aydogdu Y., Turabi A.S., Aydogdu A., Kok M. Yakinci Z. D., Karaca H.E., The effects of boron addition on the magnetic and mechanical properties of NiMnSn shape memory alloys, *Journal of Thermal Analysis and Calorimetry*, 2016, 126:399–406.
16. Vishnoi R., Singhal R. and Kaur D., Thickness dependent phase transformation of magnetron-sputtered Ni–Mn–Sn ferromagnetic shape memory alloy thin films, *Journal of Nanoparticle Research*, 2011, 13(9); 3975-3990.
17. Modak R., Deka B., Singh A.K., Gayen A., Perumal A., Manivel Raja M. and Srinivasan A., Structural And Magnetic Properties Of Ni-Mn-Sn Thin Films, *Solid State Physics*, 2015, 1665, 080072-1–080072-3.